# Higher-order effects in rarefied channel flows

Henning Struchtrup*
*Department of Mechanical Engineering, University of Victoria, Victoria BC, Canada V8W 2Y2*

Manuel Torrilhon†
*ETH Zürich, Seminar for Applied Mathematics, CH-8092 Zürich, Switzerland*
(Received 28 June 2008; published 1 October 2008)

The regularized 13 moment (R13) equations and their boundary conditions are considered for plane channel flows. Chapman-Enskog scaling based on the Knudsen number is used to reduce the equations. The reduced equations yield second-order slip conditions, and allow us to describe the characteristic dip in the temperature profile observed in force driven flow. Due to the scaling, the R13 equations' ability to describe Knudsen layers is lost. Solutions with Knudsen layers are discussed as well, and it is shown that these give a better match to direct solutions of the Boltzmann equations than the reduced equations without Knudsen layers. For a radiatively heated gas the R13 equations predict a dependence of the average gas temperature on the Knudsen number with a distinct minimum around Kn=0.2, similar to the well-known Knudsen minimum for Poiseuille flow.

DOI: 10.1103/PhysRevE.78.046301 PACS number(s): 47.10.ab, 51.10.+y, 47.45.Gx, 05.70.Ln

## I. INTRODUCTION

It is well known that the classical equations of hydrodynamics, the Navier-Stokes and Fourier laws, fail to properly describe rarefaction effects that can be observed in gases with finite Knudsen numbers. The Boltzmann equation describes the gas in microscopic detail [1–4], and by careful analysis of the equation, often involving asymptotic expansions, a wealth of rarefaction phenomena results, which can also be observed in numerical solutions of the Boltzmann equation, or from molecular dynamics.

Already for plane channel flows, such as Couette or Poiseuille flow, interesting phenomena are observed which cannot be predicted by classical hydrodynamics. We list the most significant rarefaction effects below.

(a) A heat flux in flow direction not driven by temperature gradient, while in hydrodynamics heat flux is only driven by the temperature gradient [5–9].

(b) In Couette and Poiseuille flow the pressure profile is not constant, while it is constant in classical hydrodynamics [8–12].

(c) The mass flow in Poiseuille flow as a function of the Knudsen number exhibits a minimum for Knudsen numbers around unity. This so-called Knudsen paradox cannot be described by classical hydrodynamics with first-order slip boundary conditions [13–15], but only with second-order slip conditions [16–18].

(d) The temperature profile in Poiseulle flow exhibits a characteristic dip, while classical hydrodynamics predicts a fourth-order power law and no dip [9–12,19–22].

(e) All hydrodynamic quantities (density, temperature, velocity, pressure tensor, heat flux) exhibit Knudsen boundary layers at walls [3,15,23].

(f) Phase speed and attenuation of high-frequency sound waves differ from the prediction of classical hydrodynamics [24].

(g) The detailed structure of shock waves cannot be reproduced by classical hydrodynamics [25–27].

With the classical hydrodynamic equations being unable to describe these effects, and numerical solutions of the Boltzmann equation being time expensive, a classical question in rarefied gas dynamics is whether other macroscopic transport equations can serve to properly describe rarefied gas flows.

The derivation of the Navier-Stokes and Fourier laws by means of the first-order Chapman-Enskog expansion was one of the early successes of kinetic theory [1,2]. However, the extension to higher orders leads to the Burnett [28] and super-Burnett equations [29], which are unstable [30–32]; see [33–35] for attempts to stabilize the equations. Moreover, the Chapman-Enskog method, which relies on an asymptotic expansion of the Boltzmann equation in the Knudsen number, is not appropriate for Knudsen layers, and thus the Burnett and super-Burnett equations do not properly describe these. For more details on Burnett-type equations see [4,36].

Grad's moment method [37,38] leads to stable equations at higher orders and can describe Knudsen layers [4,39,40], but, due to the hyperbolic character of the equations, shock structure calculations show spurious subshocks [41].

The biggest obstacle to the Chapman-Enskog and Grad approaches is the lack of suitable boundary conditions for the various sets of equations, which therefore cannot be applied to boundary value problems.

The regularized 13 moment (R13) equations are a macroscopic set of transport equations of third order in the Knudsen number Kn in the Chapman-Enskog sense (i.e., of super-Burnett order) that combine the benefits of Grad-type moment equations and Burnett-type equations, while omitting their problems.

The R13 equations were derived and discussed in previous contributions [38,42–45], and we state their main features [4,43,44].

The R13 equations

(a) are derived in a rational manner from the Boltzmann equation [4,43,45],

*struchtr@uvic.ca
†matorril@math.ethz.ch

 ©2008 The American Physical Society

(b) are of third order in the Knudsen number in the Chapman-Enskog sense [4,43,45],

(c) contain the classical Burnett and super-Burnett equations asymptotically [4,43,45],

(d) are linearly stable for initial and boundary value problems [4,43,45],

(e) predict phase speeds and damping of ultrasound waves in excellent agreement to experiments for Knudsen numbers below unity [4,43],

(f) give smooth shock structures for all Mach numbers, with good agreement to Direct Simulation Monte Carlo (DSMC) computations for $\mathrm{Ma}<3$ [44],

(g) exhibit Knudsen boundary layers in good agreement to DSMC simulations [43,46],

(h) are now furnished with a complete theory of boundary conditions [47,48], and

(i) obey an H-theorem for the linear case, including the boundary conditions [49].

With this, the R13 equations currently represent the only extended hydrodynamic model at Burnett or super-Burnett order that is accessible to analytical and numerical solutions of boundary value problems. So far, the solutions show excellent agreement with DSMC simulations for Knudsen numbers below unity [47,50]. In particular, as becomes evident from the literature cited above, the R13 equations exhibit typical rarefaction phenomena such as temperature and velocity slip at boundaries, heat flux not driven by temperature gradient, anisotropic normal stresses, and Knudsen layers. Further simulations and comparison to solutions of the Boltzmann equation are in preparation.

In the present paper, we further study the R13 equations for boundary value problems. First, to form the base for the discussion, we present the R13 equations for steady state plane channel flows in Sec. II. In Sec. III we shall consider a reduced form of the R13 equations that does not include Knudsen layers. It will be seen that terms of super-Burnett order give rise to (a) second-order slip boundary conditions with numerical factors close to those found in the literature [16–18], and (b) to the characteristic dip in the temperature profile that is observed in force driven Poiseuille flow [9–12,19–22]. Comparison with numerical solutions of the Boltzmann equation [15] shows that the R13 equations predict the Knudsen minimum in Poiseuille flow [13,14] for the mass flow better than the Navier-Stokes equations with second-order slip coefficients. In Sec. IV the complete linear R13 equations are solved to discuss Knudsen layers. We show that, due to the boundary conditions, the Knudsen layer amplitudes are of first order in the Knudsen number. Analytical solutions are compared to DSMC simulations, and the abilities and limitations of the R13 equations to accurately describe Knudsen layers are discussed. Finally, in Sec. V, we show that for a gas heated by absorption of radiation the average temperature as function of the Knudsen number is nonmonotonous with a minimum around $\mathrm{Kn}=0.2$. This behavior is the analogue to the Knudsen minimum for Poiseuille flow.

## II. R13 EQUATIONS FOR CHANNELS

We consider plane channel flows between two infinite, parallel plates in distance $L$, at steady state. The flow is driven by the specific body force $G_1$ which acts in the direction of the walls, or by the movement of the walls within their planes. Moreover, the gas might be heated by absorption of radiation, described through the specific absorption rate $S$. All quantities in the equations below are made dimensionless with equilibrium pressure $p_0=\rho_0\theta_0$, equilibrium temperature (in energy units) $\theta_0$, and channel distance $L$. This leads to the occurrence of the Knudsen number $\mathrm{Kn}=\frac{\mu_0\sqrt{\theta_0}}{p_0 L}$ where $\mu_0$ is the viscosity at equilibrium conditions. In equilibrium the dimensionless moments assume the values $\rho=p=\theta=1$, $v=\sigma_{ij}=q_i=\Delta=R_{ij}=m_{ijk}=0$, and the dimensionless viscosity becomes $\mu=1$. The dimensionless coordinate system is chosen such that the origin is in the center, and the plates are located at $y=\pm\frac{1}{2}$.

### A. Full R13 equations for channel flow

Under the prescribed geometry, the R13 equations for monatomic ideal gases [4,45] reduce to the following set of balance equations for dimensionless mass density $\rho$, velocity $v$, temperature $\theta$, stress components $\sigma_{12},\sigma_{11},\sigma_{22}$ and heat flux components $q_1$, $q_2$:

$$\frac{\partial\sigma_{12}}{\partial y}=\rho G_1,$$

$$p+\sigma_{22}=P_0,$$

$$\frac{\partial q_2}{\partial y}=\rho S-\sigma_{12}\frac{\partial v_1}{\partial y},$$

$$\frac{8}{5}\sigma_{12}\frac{\partial v_1}{\partial y}+\frac{\partial m_{112}}{\partial y}=-\frac{1}{\mathrm{Kn}}\frac{p}{\mu}\sigma_{11},$$

$$\frac{2}{5}\frac{\partial q_1}{\partial y}+P_0\frac{\partial v_1}{\partial y}+\frac{\partial m_{122}}{\partial y}=-\frac{1}{\mathrm{Kn}}\frac{p}{\mu}\sigma_{12},$$

$$-\frac{6}{5}\sigma_{12}\frac{\partial v_1}{\partial y}+\frac{\partial m_{222}}{\partial y}=-\frac{1}{\mathrm{Kn}}\frac{p}{\mu}\sigma_{22},$$

$$\frac{7}{5}q_2\frac{\partial v_1}{\partial y}+\frac{7}{2}\sigma_{12}\frac{\partial\theta}{\partial y}+\frac{1}{2}\frac{\partial R_{12}}{\partial y}+m_{112}\frac{\partial v_1}{\partial y}+\theta\frac{\partial\sigma_{12}}{\partial y}-\frac{\sigma_{11}}{\rho}\frac{\partial\sigma_{12}}{\partial y}=-\frac{2}{3}\frac{1}{\mathrm{Kn}}\frac{p}{\mu}q_1,$$

$$\frac{5}{2}P_0\frac{\partial\theta}{\partial y}+\theta\frac{\partial\sigma_{22}}{\partial y}+\sigma_{22}\frac{\partial\theta}{\partial y}+\frac{2}{5}q_1\frac{\partial v_1}{\partial y}+\frac{1}{2}\frac{\partial R_{22}}{\partial y}+\frac{1}{6}\frac{\partial\Delta}{\partial y}+m_{122}\frac{\partial v_1}{\partial y}-\frac{\sigma_{12}}{\rho}\frac{\partial\sigma_{12}}{\partial y}=-\frac{2}{3}\frac{1}{\mathrm{Kn}}\frac{p}{\mu}q_2. \quad (1)$$

The above equations contain the additional quantities $\Delta$, $R_{ij}$, $m_{ijk}$, that vanish in Grad's classical 13 moment equations [37,38], while in the R13 theory they obey the constitutive laws [4,45],

$$\Delta = -\frac{2}{\rho}(\sigma_{12}^2 + \sigma_{11}^2 + \sigma_{22}^2 + \sigma_{11}\sigma_{22}) - 12\,\mathrm{Kn}\frac{\mu}{p}\left(\theta\frac{\partial q_2}{\partial y} + \frac{7}{2}q_2\frac{\partial\theta}{\partial y} - \frac{q_2}{\rho}\frac{\partial p}{\partial y} + \theta\sigma_{12}\frac{\partial v}{\partial y}\right),$$

$$R_{12} = -\frac{4}{7}\frac{1}{\rho}\sigma_{12}(\sigma_{11}+\sigma_{22}) - \frac{12}{5}\mathrm{Kn}\frac{\mu}{p}\left(\theta\frac{\partial q_1}{\partial y} + 2q_1\frac{\partial\theta}{\partial y} - \frac{q_1}{\rho}\frac{\partial p}{\partial y} + \frac{5}{7}\theta(\sigma_{11}+\sigma_{22})\frac{\partial v}{\partial y}\right),$$

$$R_{22} = -\frac{4}{21}\frac{1}{\rho}(\sigma_{12}^2 + \sigma_{22}^2 - 2\sigma_{11}^2 - 2\sigma_{11}\sigma_{22}) - \frac{16}{5}\mathrm{Kn}\frac{\mu}{p}\left(\theta\frac{\partial q_2}{\partial y} + q_2\frac{\partial\theta}{\partial y} - \theta q_2\frac{\partial \ln\rho}{\partial y} + \frac{5}{14}\theta\sigma_{12}\frac{\partial v}{\partial y}\right),$$

$$m_{112} = -\frac{2}{3}\mathrm{Kn}\frac{\mu}{p}\left[\theta\left(\frac{\partial\sigma_{11}}{\partial y} - \frac{2}{5}\frac{\partial\sigma_{22}}{\partial y}\right) + \left(\sigma_{11} - \frac{2}{5}\sigma_{22}\right)\frac{\partial\theta}{\partial y} - \left(\sigma_{11} - \frac{2}{5}\sigma_{22}\right)\frac{1}{\rho}\frac{\partial p}{\partial y} + \frac{16}{25}\frac{\partial v}{\partial y}q_1\right],$$

$$m_{122} = -\frac{16}{15}\mathrm{Kn}\frac{\mu}{p}\left(\theta\frac{\partial\sigma_{12}}{\partial y} + \sigma_{12}\frac{\partial\theta}{\partial y} - \frac{\sigma_{12}}{\rho}\frac{\partial p}{\partial y} + \frac{2}{5}\frac{\partial v}{\partial y}q_2\right),$$

$$m_{222} = -\frac{6}{5}\mathrm{Kn}\frac{\mu}{p}\left(\theta\frac{\partial\sigma_{22}}{\partial y} + \sigma_{22}\frac{\partial\theta}{\partial y} - \frac{\sigma_{22}}{\rho}\frac{\partial p}{\partial y} - \frac{4}{15}\frac{\partial v}{\partial y}q_1\right). \tag{2}$$

By Chapman-Enskog expansion it can be shown that Grad's 13 moment equations lead to the Burnett equations, while the R13 equations lead to the super-Burnett equations [4]. Therefore, the above equations for $\Delta$, $R_{ij}$, $m_{ijk}$ describe super-Burnett effects.

A full set of boundary conditions for the R13 equations, derived from the boundary conditions for the Boltzmann equation, was recently presented [47], where the following relations were found (in dimensionless form)

$$\sigma_{12} = -\frac{\chi_1}{2-\chi_1}\sqrt{\frac{2}{\pi\theta}}\left(P(v_1 - v_1^W) + \frac{1}{5}q_1 + \frac{1}{2}m_{122}\right)n_2, \tag{3a}$$

$$q_2 = -\frac{\chi_2}{2-\chi_2}\sqrt{\frac{2}{\pi\theta}}\left(2P(\theta-\theta_W) - \frac{1}{2}PV^2 + \frac{1}{2}\theta\sigma_{22} + \frac{1}{15}\Delta + \frac{5}{28}R_{22}\right)n_2, \tag{3b}$$

$$m_{222} = \frac{\chi_3}{2-\chi_3}\sqrt{\frac{2}{\pi\theta}}\left(\frac{2}{5}P(\theta-\theta_W) - \frac{3}{5}PV^2 - \frac{7}{5}\theta\sigma_{22} + \frac{1}{75}\Delta - \frac{1}{14}R_{22}\right)n_2, \tag{3c}$$

$$R_{12} = \frac{\chi_4}{2-\chi_4}\sqrt{\frac{2}{\pi\theta}}\left(P\theta(v_1 - v_1^W) - \frac{11}{5}q_1 - \frac{1}{2}\theta m_{122} - PV^3 + 6PV(\theta-\theta_W)\right)n_2, \tag{3d}$$

$$m_{112} = -\frac{\chi_5}{2-\chi_5}\sqrt{\frac{2}{\pi\theta}}\left(\frac{1}{14}R_{11} + \theta\sigma_{11} - \frac{1}{5}\theta\sigma_{22} + \frac{1}{5}P(\theta-\theta_W) - \frac{4}{5}PV^2 + \frac{1}{150}\Delta\right)n_2. \tag{3e}$$

Here, $v_1^W$ and $\theta_W$ are the (dimensionless) velocity and temperature of the wall, $\chi_i$ are accommodation coefficients, and $P=\rho\theta+\frac{1}{2}\sigma_{22}-\frac{1}{120}\frac{\Delta}{\theta}-\frac{1}{28}\frac{R_{22}}{\theta}$; $n_2$ is the wall normal, pointing into the gas.

In our dimensionless variables the overall mass in the channel is unity, which implies the additional boundary condition

$$\int_{-1/2}^{1/2}\rho dy = \int_{-1/2}^{1/2}\frac{p}{\theta}dy = 1.$$

For a detailed discussion of the difficulties associated with solving boundary value problems for the nonlinear R13 equations we refer the reader to Ref. [47]. We also mention work by Gu and Emerson [48,52] who solve the R13 equations numerically with similar boundary conditions, but observe spurious boundary layers which must be attributed to the fact that they prescribe a larger number of boundary conditions than mathematically required [47].

The above boundary conditions are sufficient for linear [49] and semilinear [50] problems, and for the problems discussed below.

### B. Linearized R13 equations for channel flow

Quite often, the deviations from the ground state are small, and it suffices to consider linear equations. These are obtained by ignoring all terms in the above equations that are nonlinear in deviations from the reference state. If this is done, the equations uncouple to some degree and can be summarized into the following three sets [49,50].

(i) Velocity problem,

$$\frac{\partial\sigma_{12}}{\partial y} = G_1, \quad \frac{\partial v_1}{\partial y} + \frac{2}{5}\frac{\partial q_1}{\partial y} = -\frac{1}{\mathrm{Kn}}\sigma_{12},$$

$$\frac{1}{2}\frac{\partial R_{12}}{\partial y} + G_1 = -\frac{2}{3}\frac{1}{\mathrm{Kn}}q_1, \quad R_{12} = -\frac{12}{5}\mathrm{Kn}\frac{\partial q_1}{\partial y},$$

$$m_{122} = -\frac{16}{15}\mathrm{Kn}\, G_1, \tag{4}$$

with the boundary conditions

$$\sigma_{12} = -\frac{\chi_1}{2-\chi_1}\sqrt{\frac{2}{\pi}}\left(v_1 - v_1^W + \frac{1}{5}q_1 + \frac{1}{2}m_{122}\right)n_2,$$

$$R_{12} = \frac{\chi_4}{2-\chi_4}\sqrt{\frac{2}{\pi}}\left(v_1 - v_1^W - \frac{11}{5}q_1 - \frac{1}{2}m_{122}\right)n_2. \tag{5}$$

(ii) Temperature problem,

$$\frac{\partial q_2}{\partial y} = S,$$

$$\frac{5}{2}\frac{\partial \theta}{\partial y} + \frac{\partial \sigma_{22}}{\partial y} + \frac{1}{2}\frac{\partial R_{22}}{\partial y} + \frac{1}{6}\frac{\partial \Delta}{\partial y} = -\frac{2}{3}\frac{1}{\mathrm{Kn}}q_2,$$

$$\frac{\partial m_{222}}{\partial y} = -\frac{1}{\mathrm{Kn}}\sigma_{22},$$

$$m_{222} = -\frac{6}{5}\mathrm{Kn}\frac{\partial \sigma_{22}}{\partial y}, \quad R_{22} = -\frac{16}{5}\mathrm{Kn}\frac{\partial q_2}{\partial y}, \quad \Delta = -12\,\mathrm{Kn}\frac{\partial q_2}{\partial y}, \tag{6}$$

with the boundary conditions

$$q_2 = -\frac{\chi_2}{2-\chi_2}\sqrt{\frac{2}{\pi}}\left(2(\theta-\theta_W) + \frac{1}{2}\sigma_{22} + \frac{1}{15}\Delta + \frac{5}{28}R_{22}\right)n_2,$$

$$m_{222} = \frac{\chi_3}{2-\chi_3}\sqrt{\frac{2}{\pi}}\left(\frac{2}{5}(\theta-\theta_W) - \frac{7}{5}\sigma_{22} + \frac{1}{75}\Delta - \frac{1}{14}R_{22}\right)n_2. \tag{7}$$

(iii) The remaining equations serve to compute $p$, $\sigma_{11}$, and $m_{112}$,

$$p + \sigma_{22} = P_0,$$

$$\frac{\partial m_{112}}{\partial y} = -\frac{1}{\mathrm{Kn}}\sigma_{11}, \quad m_{112} = -\frac{2}{3}\mathrm{Kn}\left(\frac{\partial \sigma_{11}}{\partial y} - \frac{2}{5}\frac{\partial \sigma_{22}}{\partial y}\right), \tag{8}$$

with the boundary conditions

$$m_{112} = -\frac{\chi_5}{2-\chi_5}\sqrt{\frac{2}{\pi}}\left(\frac{1}{14}R_{11} + \sigma_{11} - \frac{1}{5}\sigma_{22} + \frac{1}{5}(\theta-\theta_W) + \frac{1}{150}\Delta\right)n_2,$$

$$\int_{-1/2}^{1/2}\frac{p}{\theta}dy = 1. \tag{9}$$

## III. CHAPMAN-ENSKOG SCALING

### A. Second-order equations

We shall now reduce the above equations based on the Chapman-Enskog order of magnitude of the moments, in the same manner as in Ref. [46] for Grad's 13 moment equations. We emphasize that this procedure will eliminate all Knudsen layer contributions from the equations. The full R13 equations including the Knudsen layers are discussed in Secs. IV and V below, see also Refs. [4,46,49,50].

The scales for the nonequilibrium quantities $\phi = \{\sigma_{ij}, \Delta, R_{ij}, m_{ijk}\}$ are obtained from a Chapman-Enskog expansion of the above equations. To this end we set $\phi = \phi_0 + \mathrm{Kn}\,\phi_1 + \mathrm{Kn}^2\,\phi_2 + \mathrm{Kn}^3\,\phi_3 + \cdots$ where $\phi_\alpha$ are the expansion coefficients. We are not interested in the details of the expansion coefficients, but only in the leading order of the moments. A quantity $\phi$ is said to be of $n$th order in Kn if the expansion coefficients at all orders below $n$ vanish, $\phi_\alpha = 0$ for $\alpha < n$. A $n$th-order quantity is then rescaled as $\phi = \mathrm{Kn}^n\,\tilde{\phi}$ where the rescaled value $\tilde{\phi}$ is of order unity. This will make all scales in the equations explicit.

To simplify the procedure, we assume that body force $G_1$ and absorption rate $S$ scale like the Knudsen number,

$$G_1 = \mathrm{Kn}\,\tilde{G}_1, \quad S = \mathrm{Kn}\,\tilde{S}.$$

The equilibrium quantities temperature, pressure, and velocity are not expanded, they are of zeroth order. Only shear stress and heat flux normal to the wall turn out to be first-order quantities,

$$\sigma_{12} = \mathrm{Kn}\,\tilde{\sigma}_{12}, \quad q_2 = \mathrm{Kn}\,\tilde{q}_2. \tag{10}$$

Normal stresses, normal heat flux, and some of the higher moments are of second order,

$$\sigma_{11} = \mathrm{Kn}^2\,\tilde{\sigma}_{11}, \quad \sigma_{22} = \mathrm{Kn}^2\,\tilde{\sigma}_{22}, \quad q_1 = \mathrm{Kn}^2\,\tilde{q}_1,$$

$$\Delta = \mathrm{Kn}^2\,\tilde{\Delta}, \quad R_{22} = \mathrm{Kn}^2\,\tilde{R}_{22}, \quad m_{122} = \mathrm{Kn}^2\,\tilde{m}_{122}, \tag{11}$$

while the remaining nonequilibrium quantities are of third order,

$$R_{12} = \mathrm{Kn}^3\,\tilde{R}_{12}, \quad m_{222} = \mathrm{Kn}^3\,\tilde{m}_{222}, \quad m_{112} = \mathrm{Kn}^3\,\tilde{m}_{112}. \tag{12}$$

When the rescaled variables are introduced into the R13 equations, it is straightforward to reduce these so that only terms up to second order are retained. As an example we consider the equation for the normal heat flux $q_2$ which in the rescaled variables assumes the form

$$\frac{5}{2}p\frac{\partial \theta}{\partial y} + \mathrm{Kn}^2\left(\frac{7}{2}\tilde{\sigma}_{22}\frac{\partial \theta}{\partial y} + \theta\frac{\partial \tilde{\sigma}_{22}}{\partial y} + \frac{2}{5}\tilde{q}_1\frac{\partial v_1}{\partial y} + \frac{1}{2}\frac{\partial \tilde{R}_{22}}{\partial y} + \frac{1}{6}\frac{\partial \tilde{\Delta}}{\partial y} + \tilde{m}_{122}\frac{\partial v_1}{\partial y} - \frac{\tilde{\sigma}_{12}}{\rho}\frac{\partial \tilde{\sigma}_{12}}{\partial y}\right) = -\frac{2}{3}\frac{p}{\mu}\tilde{q}_2. \tag{13}$$

Since $q_2$ is of first order in Kn, the expression $\mathrm{Kn}^2(\cdots)$ in the above equation for $\tilde{q}_2$ describes a third-order correction to $q_2$ and can be ignored in a second-order theory, so that the equation reduces to Fourier's law, $\tilde{q}_2 = -\frac{15}{4}\mu\frac{\partial \theta}{\partial y}$ to second-order accuracy. We shall later also consider the third-order terms in Eq. (13) which are responsible for the dip in the temperature profile [9–12,19–22].

To second order, our equations reduce to the conservation laws ($P_0$ is a constant of integration)

$$\frac{\partial \tilde{\sigma}_{12}}{\partial y} = \rho \tilde{G}_1, \quad p + \mathrm{Kn}^2\, \tilde{\sigma}_{22} = P_0, \quad \frac{\partial \tilde{q}_2}{\partial y} = \rho \tilde{S} - \tilde{\sigma}_{12}\frac{\partial v}{\partial y}, \tag{14}$$

the laws of Navier-Stokes and Fourier for shear stress and normal heat flux,

$$\tilde{\sigma}_{12} = -\mu \frac{\partial v_1}{\partial y}, \quad \tilde{q}_2 = -\frac{15}{4}\mu \frac{\partial \theta}{\partial y}, \tag{15}$$

and the equations for the second-order quantities (11), which we can rewrite, using (15), as

$$\tilde{\sigma}_{11} = \frac{8}{5}\frac{\tilde{\sigma}_{12}\tilde{\sigma}_{12}}{p}, \quad \tilde{\sigma}_{22} = -\frac{6}{5}\frac{\tilde{\sigma}_{12}\tilde{\sigma}_{12}}{p},$$

$$\tilde{q}_1 = -\frac{3}{2}\frac{\mu\theta}{p}\frac{\partial \tilde{\sigma}_{12}}{\partial y} + \frac{7}{2}\frac{\tilde{\sigma}_{12}\tilde{q}_2}{p},$$

$$\tilde{\Delta} = -12\frac{\mu\theta}{p}\frac{\partial \tilde{q}_2}{\partial y} + \frac{56}{5}\frac{\tilde{q}_2\tilde{q}_2}{p} + 10\frac{\theta}{p}\tilde{\sigma}_{12}\tilde{\sigma}_{12},$$

$$\tilde{R}_{22} = -\frac{16}{5}\frac{\mu\theta}{p}\frac{\partial \tilde{q}_2}{\partial y} + \frac{128}{75}\frac{\tilde{q}_2\tilde{q}_2}{p} + \frac{20}{21}\frac{\theta}{p}\tilde{\sigma}_{12}\tilde{\sigma}_{12},$$

$$\tilde{m}_{122} = -\frac{16}{15}\frac{\mu\theta}{p}\frac{\partial \tilde{\sigma}_{12}}{\partial y} + \frac{32}{45}\frac{\tilde{\sigma}_{12}\tilde{q}_2}{p}. \tag{16}$$

Equations for the third-order quantities (12) will not be required further, and are not shown.

We repeat that the complete R13 equations describe Knudsen layers [49,47,46,50], which do not obey Chapman-Enskog scaling [39]. The above reduction removes the Knudsen layer solutions. Thus, the above equations are valid in the bulk, or when Knudsen layers can be ignored, in particular in strongly nonlinear flow regimes.

### B. Second-order jump and slip boundary conditions

From the result of the scaling procedure in the preceding section we see that even to second order the R13 equations reduce to the conservation laws for momentum and energy with the Navier-Stokes and Fourier laws, with additional equation for normal stress and parallel heat flux. As we shall see now, super-Burnett effects come into play through the boundary conditions. For the reduced equations (14) and (15), we require the boundary conditions for velocity slip and temperature jump (3a) and (3b).

To be consistent with the Chapman-Enskog scaling applied before, we need to approximate the boundary conditions up to second order in Kn. To this end we introduce the rescaled quantities $\tilde{\phi}$ into the boundary conditions. For consistent scaling, velocity slip and temperature jump must be rescaled as

$$v_1 - v_1^W = \mathrm{Kn}\, \mathcal{V}, \quad \theta - \theta_W = \mathrm{Kn}\, \mathcal{T},$$

where $\mathcal{V}$ and $\mathcal{T}$ are of order unity. Then, it is straightforward to remove higher-order terms and obtain the jump and slip conditions to second order as

$$\mathcal{V} = -\frac{2-\chi_1}{\chi_1}\sqrt{\frac{\pi\theta}{2}}\frac{\tilde{\sigma}_{12}}{p}n_2 - \frac{1}{5}\mathrm{Kn}\frac{\tilde{q}_1}{p} - \frac{1}{2}\mathrm{Kn}\frac{\tilde{m}_{122}}{p},$$

$$\mathcal{T} = -\frac{2-\chi_2}{\chi_2}\sqrt{\frac{\pi\theta}{2}}\frac{\tilde{q}_2}{2p}n_2 + \frac{1}{4}\mathrm{Kn}\,\mathcal{V}^2 - \frac{1}{4}\theta\,\mathrm{Kn}\frac{\tilde{\sigma}_{22}}{p} - \frac{1}{60}\mathrm{Kn}\frac{\tilde{\Delta}}{p} - \frac{5}{56}\mathrm{Kn}\frac{\tilde{R}_{22}}{p}.$$

Not surprisingly, the second-order boundary conditions require contributions from the higher moments. It is quite remarkable, however, that the moments $\tilde{m}_{122}$, $\tilde{\Delta}$, $\tilde{R}_{22}$ are required, which contribute terms of super-Burnett order to the transport equations, but terms of Burnett order to the boundary conditions.

Now we can insert our constitutive equations for higher moments (16), and also we use the slip condition for the square of the slip in the second one to obtain

$$\mathcal{V} = -\frac{2-\chi_1}{\chi_1}\sqrt{\frac{\pi\theta}{2}}\frac{\tilde{\sigma}_{12}}{p}n_2 + \frac{5}{6}\mathrm{Kn}\frac{\mu\theta}{p^2}\frac{\partial \tilde{\sigma}_{12}}{\partial y} - \frac{19}{18}\mathrm{Kn}\frac{\tilde{\sigma}_{12}\tilde{q}_2}{p^2}, \tag{17}$$

$$\mathcal{T} = -\frac{2-\chi_2}{\chi_2}\sqrt{\frac{\pi\theta}{2}}\frac{\tilde{q}_2}{2p}n_2 + \frac{17}{35}\mathrm{Kn}\frac{\mu\theta}{p^2}\frac{\partial \tilde{q}_2}{\partial y} + \mathrm{Kn}\left[\frac{\pi}{8}\left(\frac{2-\chi_1}{\chi_1}\right)^2 + \frac{71}{1470}\right]\theta\frac{\tilde{\sigma}_{12}\tilde{\sigma}_{12}}{p^2} - \mathrm{Kn}\frac{178}{525}\frac{\tilde{q}_2\tilde{q}_2}{p^2}. \tag{18}$$

Second-order slip and jump conditions are widely available in the literature. For comparison we focus on the slip condition (17), in which we introduce the Navier-Stokes and Fourier laws (15), so that in the standard dimensionless quantities it assumes the form

$$v_1 - v_1^W = \frac{2-\chi_1}{\chi_1}\mathrm{Kn}\sqrt{\frac{\pi\theta}{2}}\frac{\mu}{p}\frac{\partial v_1}{\partial y}n_2 - \frac{5}{6}\mathrm{Kn}^2\frac{\mu^2}{p^2}\frac{\theta\partial^2 v_1}{\partial y^2} - \mathrm{Kn}^2\frac{\mu^2}{p^2}\left(\frac{5}{6}\frac{d\ln\mu}{d\ln\theta} + \frac{95}{24}\mathrm{Kn}^2\frac{\mu^2}{p^2}\right)\frac{\partial\theta}{\partial y}\frac{\partial v_1}{\partial y}.$$

For slow flows, one might ignore the nonlinear term, so that

$$v_1 - v_1^W = \alpha\,\mathrm{Kn}\sqrt{\frac{\pi\theta}{2}}\frac{\mu}{p}\frac{\partial v_1}{\partial y}n_2 - \beta\,\mathrm{Kn}^2\frac{\mu^2}{p^2}\frac{\theta\partial^2 v_1}{\partial y^2}, \tag{19}$$

with $\alpha = \frac{2-\chi_1}{\chi_1}$ and $\beta = \frac{5}{6}$. The following table shows values for the second-order slip coefficient $\beta$ taken from different authors for the case of full accommodation ($\chi_1 = 1$),

| R13 (this paper) | Deissler [16] | Hadjiconstantinou [17] | Lockerby *et al.* [18] |
|---|---|---|---|
| $\frac{5}{6}=0.833$ | $\frac{9\pi}{16}=1.767$ | $0.606\frac{\pi}{2}=0.952$ | $\frac{3}{10}=0.3$ |

We see that the value for $\beta$ from the R13 equations is quite close to the value by Hadjiconstantinou. Deisslers value seems a bit high. Lockerby *et al.* used the Burnett equation for $q_1$ in the temperature jump condition (3b), but missed the super-Burnett contribution of $m_{122}$. For the case of full accommodation ($\chi_1=1$), all cited authors report a value $\alpha=1$, only Hadjiconstantinou reports a corrected slip coefficient $\alpha_H=1.1466$ [17].

### C. Knudsen paradox

In order to study the second-order slip effects in a simple manner, we ignore variations of density and viscosity which are assumed to have their equilibrium values (i.e., unity in our dimensionless variables), so that the stress and velocity follow from

$$\frac{\partial\tilde{\sigma}_{12}}{\partial y}=\tilde{G}_1, \quad \tilde{\sigma}_{12}=-\frac{\partial v_1}{\partial y}, \tag{20}$$

with the boundary condition (19) ($v_W=0$, resting walls at $y=\pm\frac{1}{2}$, $\tilde{G}_1=G_1/\mathrm{Kn}$), as

$$v_1=\frac{G_1}{2\,\mathrm{Kn}}\left[\left(\frac{1}{4}-y^2\right)+\alpha\sqrt{\frac{\pi}{2}}\mathrm{Kn}+2\beta\,\mathrm{Kn}^2\right], \quad \sigma_{12}=-G_1 y. \tag{21}$$

The average mass flow rate is

$$J=\int_{-1/2}^{1/2} v_1 dy=\frac{G_1}{12\,\mathrm{Kn}}\left(1+6\alpha\,\mathrm{Kn}\sqrt{\frac{\pi}{2}}+12\beta\,\mathrm{Kn}^2\right). \tag{22}$$

The mass flow rate for the full R13 equations was computed in Ref. [49] as the solution of the velocity problem (4) and (5); the result can be written as

$$J=\frac{G_1}{12\,\mathrm{Kn}}\left[1+6\sqrt{\frac{\pi}{2}}\left(1+\frac{3\sqrt{2/\pi}}{12\sqrt{5}+25}\right)\mathrm{Kn}+12\frac{\frac{32}{\sqrt{5}}+\frac{85}{3}}{12\sqrt{5}+25}\mathrm{Kn}^2-\frac{18}{25}\mathrm{Kn}\left(\frac{(1+5\,\mathrm{Kn})^2}{\left(1+\frac{5}{12}\sqrt{5}\coth\frac{\sqrt{5}}{6\,\mathrm{Kn}}\right)}-\frac{(1+10\,\mathrm{Kn})}{\left(1+\frac{5}{12}\sqrt{5}\right)}\right)\right]. \tag{23}$$

Here, the last term contributes only terms of order $O(\mathrm{Kn}^3)$ and higher. Comparison between the second-order approximation (22) and the R13 result (23)—which includes Knudsen layers—suggests for the first- and second-order slip coefficients the values $\alpha=1+\frac{3\sqrt{2/\pi}}{12\sqrt{5}+25}=1.0462$ and $\beta=(\frac{32}{\sqrt{5}}+\frac{85}{3})/(12\sqrt{5}+25)=0.8227$.

Figure 1 compares the reduced mass flow $J/G_1$ computed from the Navier-Stokes equations with second-order slip boundary conditions (22) for a variety of slip coefficients, and the R13 equations (23), to the numerical solution of the Boltzmann equation by Ohwada *et al.* [15]. Apart from the Navier-Stokes solution with first-order slip, all curves show a minimum around $\mathrm{Kn}\simeq 0.5$. The occurence of this minimum is known as the Knudsen paradox. Clearly, the solution of the complete linear R13 equations in Ref. [49] gives the best match to the Boltzmann solution, while the reduced R13 equations derived above give numerical values for the second-order slip coefficient that lead to the best match with the full Boltzmann solution among all choices.

The solution (21) of the Navier-Stokes equation can be used to compute the other moments for Poiseuille flow (to second order, and ignoring Knudsen layer contributions).

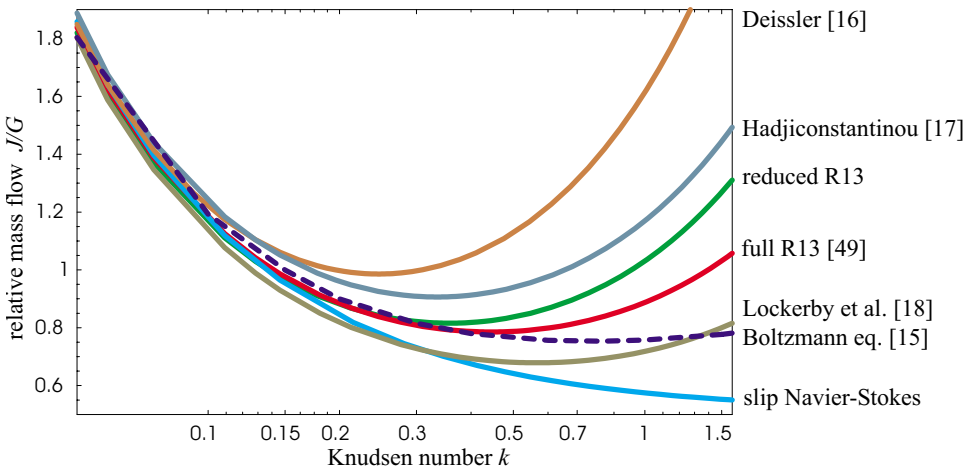


FIG. 1. (Color online) Relative mass flow rate $J/G_1$ over Ohwada's Knudsen number $k=\frac{4}{5}\sqrt{2}\mathrm{Kn}$, for Boltzmann equation (dashed line) [15], full R13 equations [49], the reduced R13 equations of the present paper, and Navier-Stokes with second-order slip conditions from Deissler [16], Hadjiconstantinou [17], and Lockerby *et al.* [18].

Linearized in $\theta$, $p$, and $\mu$ the first law reduces to

$$\frac{\partial \tilde{q}_2}{\partial y} = \tilde{\sigma}_{12}^2 = \tilde{G}_1^2 y^2 \quad \text{so that } \tilde{q}_2 = \frac{1}{3}\tilde{G}_1^2 y^3, \tag{24}$$

where the integration constant is zero due to symmetry. Within the same approximation, and considering only terms up to order $G^3$ in the driving force, we find for the higher moments (16),

$$\tilde{\sigma}_{22} = -\tfrac{6}{5}\tilde{G}_1^2 y^2, \tag{25a}$$

$$\tilde{q}_1 \simeq \tfrac{3}{2}\tilde{G}_1 - \tfrac{7}{6}\tilde{G}_1^3 y^4, \tag{25b}$$

$$\tilde{R}_{22} \simeq -\tfrac{236}{105}\tilde{G}_1^2 y^2, \tag{25c}$$

$$\tilde{\Delta} = -2\tilde{G}_1^2 y^2, \tag{25d}$$

$$\tilde{m}_{122} = -\tfrac{16}{15}\tilde{G}_1 - \tfrac{32}{135}\tilde{G}_1^3 y^4, \tag{25e}$$

### D. Temperature dip as super-Burnett effect

Now, we consider the equation for heat flux (13) where we include the third-order contributions (the factor on $\mathrm{Kn}^2$) with the results for the higher-order moments (25), to find, again up to terms in $G_1^3$,

$$\frac{\partial \theta}{\partial y} = -\frac{4}{45}\tilde{G}_1^2 y^3 + \frac{976}{525}\mathrm{Kn}^2 \tilde{G}_1^2 y.$$

Integration, and use of the jump boundary conditions (18) gives (with $\tilde{G}_1 = \frac{G_1}{\mathrm{Kn}}$)

$$\theta - \theta_W = \frac{G_1^2}{8\,\mathrm{Kn}}\left[\sqrt{\frac{\pi}{2}}\frac{1}{6} + \mathrm{Kn}\left(\frac{\pi}{4} + \frac{157}{147}\right)\right] + \frac{G_1^2}{\mathrm{Kn}^2}\left[\frac{1}{45}\left(\frac{1}{16} - y^4\right) - \frac{488}{525}\mathrm{Kn}^2\left(\frac{1}{4} - y^2\right)\right]. \tag{26}$$

Here, the first term describes the temperature jump at the wall, while the second term describes the temperature profile. The competition between the positive hydrodynamic term, $\frac{1}{45}(\frac{1}{16} - y^4)$, and the negative R13 correction, $-\frac{488}{525}\mathrm{Kn}^2(\frac{1}{4} - y^2)$, leads to the characteristic dip of the temperature profile that is widely discussed in the literature [9–12,19–22].

Based on a high accuracy expansion of the Boltzmann equation for Maxwell molecules Tij *et al.* [11] find a coefficient $C_T = 1.0153$ for the correction term in (26), instead of the R13 result $\frac{488}{525} \simeq 0.93$. However, the R13 equations agree with their results for normal stress $\tilde{\sigma}_{22}$ (25a), parallel heat flux $\tilde{q}_1$ (25b), and conductive heat flux (24). Note that these authors did not include temperature jump boundary conditions and Knudsen layers into their results.

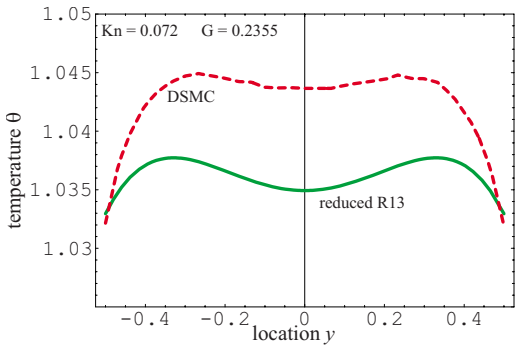


FIG. 2. (Color online) Temperature profile for force driven channel flow, DSMC result [21] and reduced R13 result, Eq. (26).

Figure 2 compares the temperature curve of Eq. (26) to DSMC data by Xu [21] for $\mathrm{Kn} = 0.072$, $G_1 = 0.2355$. The main difference between the two curves are the more pronounced shoulders at the walls in the DSMC simulation, which are due to Knudsen layers that are ignored in the present simplified analysis. Our analytic computation of the temperature profile stands in agreement with the results of Xu [21], who used his gas-kinetic scheme to solve the super-Burnett equations numerically, and recognized the dip as a super-Burnett effect. An analytical solution of the semilinearized R13 equations that includes the Knudsen layers is presented elsewhere [50].

## IV. LINEAR KNUDSEN LAYERS

Within the Chapman-Enskog scaling, we found that the moments (11) and (12), which vanish within classical hydrodynamics, are of second or higher order in the Knudsen number. However, the Chapman-Enskog scaling ignores Knudsen layers, which we study now, in order to gain further insight into their characteristics.

Knudsen layers are essentially linear effects, and thus it is sufficient to study the linearized equations.

We consider the velocity problem (4) and (5) for Couette flow between two parallel plates at $y = \pm\frac{1}{2}$ which move with the velocities $\pm v_W$ within their planes, for the force free case, $G_1 = 0$. It is straightforward to solve the equations analytically to find

$$v_1 = -\frac{v_1^W}{1 + \mathrm{Kn}\dfrac{13\sqrt{\pi/2} + 2\sqrt{5}}{6 + \sqrt{10\pi}\coth\left(\dfrac{\sqrt{5}}{6\,\mathrm{Kn}}\right)}}\left(2y + \frac{\sqrt{2\pi}\mathrm{Kn}}{6 + \sqrt{10\pi}\coth\left(\dfrac{\sqrt{5}}{6\,\mathrm{Kn}}\right)}\frac{\sinh\left(\dfrac{\sqrt{5}y}{3\,\mathrm{Kn}}\right)}{\sinh\left(\dfrac{\sqrt{5}}{6\,\mathrm{Kn}}\right)}\right),$$

$$\sigma_{12} = \frac{2\,\mathrm{Kn}\,v_1^W}{1 + \mathrm{Kn}\dfrac{13\sqrt{\pi/2} + 2\sqrt{5}}{6 + \sqrt{10\pi}\coth\left(\dfrac{\sqrt{5}}{6\,\mathrm{Kn}}\right)}},$$

$$q_1 = \frac{5\sqrt{\dfrac{\pi}{2}}\mathrm{Kn}\,v_1^W}{\left[6 + \sqrt{10\pi}\coth\left(\dfrac{\sqrt{5}}{6\,\mathrm{Kn}}\right)\right] + \mathrm{Kn}(13\sqrt{\pi/2} + 2\sqrt{5})}\frac{\sinh\left(\dfrac{\sqrt{5}y}{3\,\mathrm{Kn}}\right)}{\sinh\left(\dfrac{\sqrt{5}}{6\,\mathrm{Kn}}\right)},$$

$$R_{12} = -\frac{2\sqrt{10\pi}\mathrm{Kn}\,v_1^W}{\left[6 + \sqrt{10\pi}\coth\left(\dfrac{\sqrt{5}}{6\,\mathrm{Kn}}\right)\right] + \mathrm{Kn}(13\sqrt{\pi/2} + 2\sqrt{5})}\frac{\cosh\left(\dfrac{\sqrt{5}y}{3\,\mathrm{Kn}}\right)}{\sinh\left(\dfrac{\sqrt{5}}{6\,\mathrm{Kn}}\right)},$$

$$m_{122} = 0. \tag{27}$$

The solution for the moments $q_1$ and $R_{12}$ describe Knudsen layers with amplitudes of first order in Kn.

Before we discuss how the above compares to DSMC simulations, we have a brief look at this problem as described by conventional hydrodynamics, i.e., the Navier-Stokes theory with slip boundary conditions (19), where the following equations need to be solved:

$$\frac{\partial \sigma_{12}}{\partial y} = 0, \quad \frac{\partial v_1}{\partial y} = -\frac{1}{\mathrm{Kn}}\sigma_{12} \text{ with } v_1 - v_1^W = \alpha\,\mathrm{Kn}\sqrt{\frac{\pi}{2}}\frac{\partial v}{\partial y}n_2. \tag{28}$$

Here we introduced the Knudsen layer correction coefficient $\alpha$, as is often done in kinetic theory [2,17]. Note that for (linear) Couette flow the second-order correction in (19) does not contribute. The corresponding solution reads as

$$v^{\mathrm{NS}} = -\frac{2v_1^W y}{1 + \sqrt{2\pi}\alpha\,\mathrm{Kn}}, \quad \sigma_{12}^{\mathrm{NS}} = \frac{-2\,\mathrm{Kn}\,v_1^W}{1 + \sqrt{2\pi}\alpha\,\mathrm{Kn}}. \tag{29}$$

Figure 3 compares the above solutions for the R13 equations (27) and the Navier-Stokes equations (29) with and without Knudsen layer correction to DSMC simulations for Maxwell molecules at Kn=0.1, $v_W$=100 m/s which were obtained with Bird's code [51]; in the plots the dimensionless space coordinate $y$ is shifted by 0.5, so that the boundaries are at 0 and 1.

In the figures, the black continuous curves show the DSMC results which must be considered as the relevant benchmark. The dashed green curves show the R13 results. We notice very good agreement to the DSMC simulations. The stress $\sigma_{12}$ deviates by $\simeq 1\%$ from the DSMC result, and the parallel heat flux $q_1$ matches the DSMC curve quite accurately. The small differences in the middle are due to nonlinear effects described by (16) that are lost in the linearization. The upper left-hand figure shows the velocity for the whole domain, where all curves lie quite close to each other. To see the differences one needs to study the blow-up of the region at the left-hand wall (the upper right-hand figure), where it becomes obvious that the R13 equation cannot completely describe the details of the velocity Knudsen layer. However, while the R13 solutions exhibit a larger slip and a less pronounced Knudsen layer than the DSMC simulations, the two curves meet less than a mean free path away from the wall. Our anlytical results agree with the numerical solution by Gu and Emerson [52], which however shows some spurious layers at the walls [47].

The short-dashed red curves show the results from slip-Navier-Stokes without Knudsen layer correction ($\alpha$=1). The velocity is met quite well overall, where the differences near to the wall are more pronounced. The stress deviates by $\simeq 2\%$ from the DSMC result and, of course, classical hydrodynamics predicts a vanishing parallel heat flux $q_1$.

The dashed-dotted dark red curves show the results for slip-Navier-Stokes with Knudsen layer correction ($\alpha$=1.1), where the correction coefficient was adjusted to give the proper value for stress $\sigma_{12}$. Interestingly, the correction leads to less accurate values for the velocity close to the wall, as can be seen in the blow-up. Thus, the correction cannot be recommended.

In a previous paper [39] we have shown that the actual Knudsen layer is a linear superposition of many exponential layers $\exp(-\gamma_\alpha \frac{y}{\mathrm{Kn}})$ with a wide variety of coefficients $\gamma_\alpha$. The R13 equations give only one such contribution, and this explains why the velocity is not described accurately close to the wall.

Nevertheless, the R13 system gives an improvement over slip-Navier-Stokes, not only in increased accuracy for stress and velocity, but also in that it can describe the nonclassical heat flux $q_1$ which is a pure rarefaction effect.

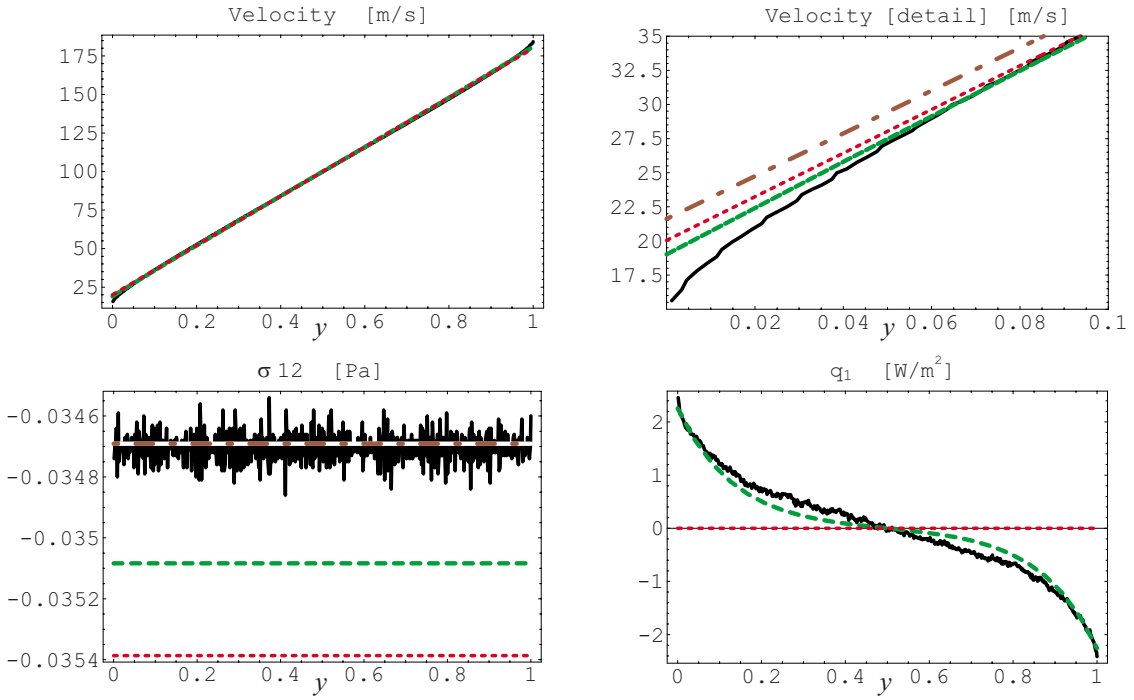


FIG. 3. (Color online) Velocity $v$, stress $\sigma_{12}$, and heat flux parallel to the flow $q_1$ for Couette flow at Kn=0.1, $v_W$=100 m/s: Continuous line (black), DSMC simulation; dashed line (green), R13 equation; short dashed line (red), Navier-Stokes with slip; dashed-dotted line (dark red), Navier-Stokes with Knudsen layer correction ($\alpha$=1.1).

Lockerby *et al.* [53] criticize the R13 equations for not being able to accurately describe the velocity Knudsen layer, see also comments by Gu and Emerson [52]. In their paper the authors fit an analytical solution to the DSMC data in order to determine the constants of integration, and did not use any boundary conditions. In their fitting they tried to fit the R13 result to the DSMC result in the Knudsen layer. Our analytical solution does not need any fitting to DSMC simulations. Although the finer details of the velocity Knudsen layers are not reproduced, the results are in rather close agreement to the simulations, since additional slip compensates the lower amplitude of the Knudsen layer.

## V. KNUDSEN PARADOX FOR TEMPERATURE IN GAS HEATED BY RADIATION

The R13 equations predict an effect similar to the Knudsen paradox for Poiseuille flow for the case of a gas heated by absorption of radiation.

We consider the linear temperature problem (6) and (7) for a gas at rest between two walls at constant temperature $\theta_W$, heated by absorption of radiative energy $S$.

Due to the symmetry of the problem, the solution for temperature can be written in terms of the local temperature difference to the walls over the absorption rate, as

$$\frac{\theta-\theta_W}{S}=\frac{2}{15}\frac{1}{\mathrm{Kn}}\left(\frac{1}{4}-y^2\right)+\frac{39}{10}\left(\sqrt{\frac{\pi}{2}}+\frac{36}{13}\mathrm{Kn}\right)+\sqrt{\frac{15}{4}\pi}\left(\sqrt{\frac{\pi}{2}}+\frac{96}{35}\mathrm{Kn}\right)\tanh\left(\sqrt{\frac{5}{6}}\frac{1}{2\,\mathrm{Kn}}\right)-\frac{2}{5}\left(\sqrt{\frac{\pi}{2}}+\frac{24}{7}\mathrm{Kn}\right)\frac{\cosh\left(\sqrt{\frac{5}{6}}\frac{y}{\mathrm{Kn}}\right)}{\cosh\left(\sqrt{\frac{5}{6}}\frac{1}{2\,\mathrm{Kn}}\right)}+\frac{}{15+2\sqrt{15\pi}\tanh\left(\sqrt{\frac{5}{6}}\frac{1}{2\,\mathrm{Kn}}\right)}, \quad (30)$$

while the other moments are given by

$$q_2 = Sy,$$

$$\sigma_{22} = S\frac{\sqrt{\frac{\pi}{2}} + \frac{24}{7}\mathrm{Kn}}{15 + 2\sqrt{15\pi}\tanh\left(\sqrt{\frac{5}{6}}\frac{1}{2\,\mathrm{Kn}}\right)}\frac{\cosh\left(\sqrt{\frac{5}{6}}\frac{y}{\mathrm{Kn}}\right)}{\cosh\left(\sqrt{\frac{5}{6}}\frac{1}{2\,\mathrm{Kn}}\right)},$$

$$m_{222} = -S\frac{\sqrt{\frac{\pi}{2}} + \frac{24}{7}\mathrm{Kn}}{15 + 2\sqrt{15\pi}\tanh\left(\sqrt{\frac{5}{6}}\frac{1}{2\,\mathrm{Kn}}\right)} \times \sqrt{\frac{6}{5}}\frac{\sinh\left(\sqrt{\frac{5}{6}}\frac{y}{\mathrm{Kn}}\right)}{\cosh\left(\sqrt{\frac{5}{6}}\frac{1}{2\,\mathrm{Kn}}\right)},$$

$$R_{22} = -\frac{16}{5}\mathrm{Kn}\,S, \quad \Delta = -12\,\mathrm{Kn}\,S.$$

As an overall measure for the heating of the gas we define the average relative temperature increase as

$$E = \int_{-1/2}^{1/2} \frac{\theta - \theta_W}{S} dy.$$

For the above result of the R13 equations (30) we obtain from integration

$$E_{\mathrm{R13}} = \frac{1}{45}\frac{1}{\mathrm{Kn}} + \frac{13}{50}\sqrt{\frac{\pi}{2}} + \frac{18}{25}\mathrm{Kn} + \frac{\sqrt{\frac{6}{5}}\left(7\pi + 160\,\mathrm{Kn}\sqrt{\frac{\pi}{2}} + 384\,\mathrm{Kn}^2\right)}{140\left(15\coth\left(\sqrt{\frac{5}{6}}\frac{1}{2\,\mathrm{Kn}}\right) + 2\sqrt{15\pi}\right)}. \quad (31)$$

For classical hydrodynamics with linear second-order slip conditions, we must solve Fourier's law

$$\frac{\partial q_2}{\partial y} = S, \quad q_2 = -\frac{15}{4}\mathrm{Kn}\frac{\partial \theta}{\partial y},$$

with the jump boundary condition (18) that reduces to

$$\theta - \theta_W = -\frac{2-\chi_2}{2\chi_2}\sqrt{\frac{\pi}{2}}q_2 n_2 + \frac{17}{35}\mathrm{Kn}\frac{\partial q_2}{\partial y}.$$

The solution reads as

$$\theta - \theta_W = \frac{2}{15}\frac{S}{\mathrm{Kn}}\left(\frac{1}{4} - y^2\right) + \frac{2-\chi_2}{\chi_2}\sqrt{\frac{\pi}{2}}\frac{S}{4} + \frac{17}{35}\mathrm{Kn}\,S,$$

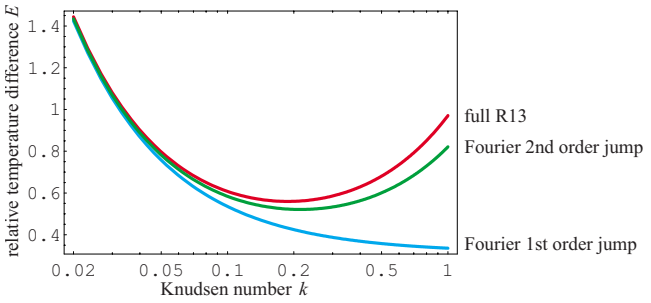


FIG. 4. (Color online) Relative temperature increase $E$ over Ohwada's Knudsen number $k = \frac{4}{5}\sqrt{2}\mathrm{Kn}$ as predicted from the linearized R13 equations.

and the relative temperature difference (for $\chi_2 = 1$) is obtained as

$$E_F = \frac{1}{45}\frac{1}{\mathrm{Kn}} + \frac{1}{4}\sqrt{\frac{\pi}{2}} + \frac{17}{35}\mathrm{Kn}. \quad (32)$$

If one considers only first-order jump conditions, the last term vanishes, so that $E_{F1} = \frac{1}{45}\frac{1}{\mathrm{Kn}} + \frac{1}{4}\sqrt{\frac{\pi}{2}}$.

Figure 4 shows the relative temperature difference $E$ as function of the Knudsen number for the full R13 solution (31), and the Fourier solutions with first- and second-order jump conditions (32). For consistency with Fig. 1, we plotted over Ohwada's Knudsen number $k$. The R13 equations predict a minimum at $k \simeq 0.2$ (or $\mathrm{Kn} = 0.18$), which is also predicted by Fourier's law with second-order jump conditions. With first-order jump conditions, however, Fourier's law does not predict a minimum. We are not aware of solutions of the Boltzmann equation or DSMC simulations for comparison, but are confident that DSMC simulations will show this minimum in good agreement to the prediction of the R13 equations, similar to their prediction of the Knudsen minimum in Fig. 1.

## VI. CONCLUSIONS

At present, the R13 equations are the only macroscopic model for rarefied gas flows at super-Burnett order with a complete set of boundary conditions. In this paper we have discussed the properties and abilities of the R13 equations for the description of plane channel flows.

By an expansion in the Knudsen number it was shown that the R13 equations and their boundary conditions can be reduced to the Navier-Stokes-Fourier equations with second-order jump and slip boundary conditions. The resulting values for the slip coefficients lead to good agreement with numerical solutions of the Boltzmann equation. The expansion removes Knudsen layer contributions from the solutions, and it was shown that the inclusion of these leads to markedly better results as compared to classical hydrodynamics with second-order slip boundary conditions.

For radiatively heated gases, the R13 equations predict the "temperature-Knudsen-paradox," i.e., a dependence of the average gas temperature on the Knudsen number with a minimum around $\mathrm{Kn} = 0.2$, similar to the well-known Knudsen minimum for Poiseuille flow.

The R13 equations with boundary conditions reproduce all known higher-order effects in rarefied gas dynamics with good accuracy. The next step is the analytical and numerical solution of flows in more complex geometries, in particular for two- and three-dimensional flows, as well as simulation of unsteady problems.

**ACKNOWLEDGMENTS**

Support by the Natural Sciences and Engineering Research Council (NSERC) and the European Science Foundation (ESF) is gratefully acknowledged. The authors thank Dr. Kun Xu (Hong Kong) for providing the DSMC data for Poiseuille flow.

[1] S. Chapman and T. G. Cowling, *The Mathematical Theory of Non-Uniform Gases* (Cambridge University Press, Cambridge, 1970).
[2] C. Cercignani, *Theory and Application of the Boltzmann Equation* (Scottish Academic Press, Edinburgh, 1975).
[3] Y. Sone, *Kinetic Theory and Fluid Dynamics* (Birkhäuser, Boston, 2002).
[4] H. Struchtrup, *Macroscopic Transport Equations for Rarefied Gas Flows—Approximation Methods in Kinetic Theory*, Interaction of Mechanics and Mathematics Series (Springer, Heidelberg, 2005).
[5] A. Baranyai, D. J. Evans, and P. J. Daivis, Phys. Rev. A **46**, 7593 (1992).
[6] B. D. Todd and D. J. Evans, J. Chem. Phys. **103**, 9804 (1995).
[7] B. D. Todd and D. J. Evans, Phys. Rev. E **55**, 2800 (1997).
[8] F. J. Uribe and A. L. Garcia, Phys. Rev. E **60**, 4063 (1999).
[9] K. Aoki, S. Takata, and T. Nakanishi, Phys. Rev. E **65**, 026315 (2002).
[10] M. Tij and A. Santos, J. Stat. Phys. **76**, 1399 (1994).
[11] M. Tij, M. Sabbane, and A. Santos, Phys. Fluids **10**, 1021 (1998).
[12] M. M. Mansour, F. Baras, and A. L. Garcia, Physica A **240**, 255 (1997).
[13] M. Knudsen, Ann. Phys. **333**, 75 (1909).
[14] K. A. Hickey and S. K. Loyalka, J. Vac. Sci. Technol. A **8**, 735 (1990).
[15] T. Ohwada, Y. Sone, and K. Aoki, Phys. Fluids A **1**, 2042 (1989).
[16] R. G. Deissler, Int. J. Heat Mass Transfer **7**, 681 (1964).
[17] N. G. Hadjiconstantinou, Phys. Fluids **15**, 2352 (2003).
[18] D. A. Lockerby, J. M. Reese, D. R. Emerson, and R. W. Barber, Phys. Rev. E **70**, 017303 (2004).
[19] M. Alaoui and A. Santos, Phys. Fluids A **4**, 1273 (1992).
[20] Y. Zheng, A. L. Garcia, and B. J. Alder, J. Stat. Phys. **109**, 495 (2002).
[21] K. Xu, Phys. Fluids **15**, 2077 (2003).
[22] K. Xu and Z. H. Li, J. Fluid Mech. **513**, 87 (2004).
[23] D. Risso and P. Cordero, Phys. Rev. E **58**, 546 (1998).
[24] M. Greenspan, J. Acoust. Soc. Am. **28**, 644 (1956).
[25] H. Alsmeyer, J. Fluid Mech. **74**, 497 (1976).
[26] D. Gilbarg and D. Paolucci, J. Rat. Mech. Anal **2**, 617 (1953).
[27] B. L. Holian, C. W. Patterson, M. Mareschal, and E. Salomons, Phys. Rev. E **47**, R24 (1993).
[28] D. Burnett, Proc. London Math. Soc. **40**, 382 (1936).
[29] M. Sh. Shavaliyev, J. Appl. Math. Mech. **57**, 573 (1993).
[30] A. V. Bobylev, Sov. Phys. Dokl. **27**, 29 (1982).
[31] P. Rosenau, Phys. Rev. A **40**, 7193 (1989).
[32] F. J. Uribe, R. M. Velasco, and L. S. García-Colín, Phys. Rev. E **62**, 5835 (2000).
[33] X. Zhong, R. W. MacCormack, and D. R. Chapman, AIAA J. **31**, 1036 (1993).
[34] A. V. Bobylev, J. Stat. Phys. **124**, 371 (2006).
[35] L. H. Söderholm, Transp. Theory Stat. Phys. **36**, 495 (2007).
[36] L. S. García-Colín, R. M. Velasco, and F. J. Uribe, Phys. Rep. **465**, 149 (2008).
[37] H. Grad, Commun. Pure Appl. Math. **2**, 331 (1949).
[38] H. Grad, "Principles of the kinetic theory of gases," in *Handbuch der Physik XII: Thermodynamik der Gase*, edited by S. Flügge (Springer, Berlin 1958).
[39] H. Struchtrup, Physica A **387**, 1750 (2008).
[40] D. Reitebuch and W. Weiss, Continuum Mech. Thermodyn. **11**, 217 (1999).
[41] W. Weiss, Phys. Rev. E **52**, R5760 (1995).
[42] I. V. Karlin, A. N. Gorban, G. Dukek, and T. F. Nonnenmacher, Phys. Rev. E **57**, 1668 (1998).
[43] H. Struchtrup and M. Torrilhon, Phys. Fluids **15**, 2668 (2003).
[44] M. Torrilhon and H. Struchtrup, J. Fluid Mech. **513**, 171 (2004).
[45] H. Struchtrup, Phys. Fluids **16**, 3921 (2004).
[46] H. Struchtrup and T. Thatcher, Continuum Mech. Thermodyn. **19**, 177 (2007).
[47] M. Torrilhon and H. Struchtrup, J. Comput. Phys. **227**, 1982 (2008).
[48] X. Gu and D. Emerson, J. Comput. Phys. **225**, 263 (2007).
[49] H. Struchtrup and M. Torrilhon, Phys. Rev. Lett. **99**, 014502 (2007).
[50] P. Taheri, M. Torrilhon, and H. Struchtrup (unpublished).
[51] G. Bird, *Molecular Gas Dynamics and the Direct Simulation of Gas Flows* (Clarendon, Oxford, 1994).
[52] X. J. Gu, R. W. Barber, and D. R. Emerson, Nanoscale Microscale Thermophys. Eng. **11**, 85 (2007).
[53] D. A. Lockerby, J. M. Reese, and M. A. Gallis, Phys. Fluids **17**, 100609 (2005).

# Erratum: Higher-order effects in rarefied channel flows [Phys. Rev. E 78, 046301 (2008)]

Henning Struchtrup and Manuel Torrilhon
(Received 19 November 2008; published 16 December 2008)

DOI: 10.1103/PhysRevE.78.069903 PACS number(s): 47.10.ab, 51.10.+y, 05.70.Ln, 99.10.Cd

Due to an unfortunate oversight, for the comparison of second-order slip models we did not properly represent the slip coefficients given by Hadjiconstaninou [1] (Ref. [17] in the original paper).

Hadjiconstaninou gives the following values for the second order slip coefficient $\beta$:

| Hadjiconstaninou [17] (uncorrected) | Hadjiconstaninou [17] (Kn-layer correction) |
|---|---|
| $0.606\frac{\pi}{2}=0.952$ | $0.31\frac{\pi}{2}=0.487$ |

where the second value is corrected for Knudsen layer effects. In the paper we used only the first value, which does not account for Knudsen layer effects. Moreover, Hadjiconstantinou reports a first order slip coefficient $\alpha_H=1.11$.

Correspondingly, the curve for Hadjiconstantinou's corrected slip coefficients must be added to Fig. 1.

Clearly, Hadjiconstannou's corrected slip coefficients give an excellent match for Knudsen numbers up to $k\simeq 0.4$. There is a close agreement between the result from the full R13 equations—which explicitly include Knudsen layers—and the curve obtained from Hadjiconstaninou's coefficients that were corrected for Knudsen layer effects.

We thank Ehsan Roohi (Sharif University of Technology, Tehran, Iran) for pointing our attention to this omission.

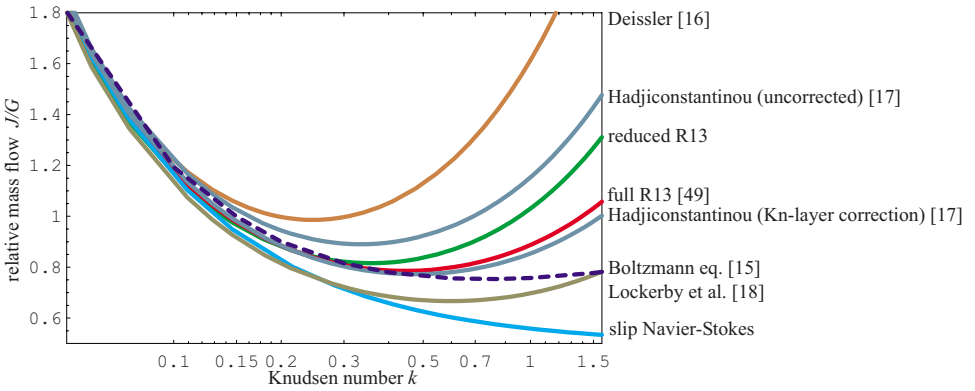


FIG. 1. (Color online) Relative mass flow rate $J/G_1$ over Ohwada's Knudsen number $k=\frac{4}{5}\sqrt{2}\mathrm{Kn}$, for Boltzmann equation (dashed line) [15], full R13 equations [49], the reduced R13 equations of the present paper, and Navier-Stokes with second-order slip conditions from Deissler [16], Hadjiconstantinou with and without Knudsen layer correction [17], and Lockerby *et al.* [18].

[1] N. G. Hadjiconstantinou, Phys. Fluids **15**, 2352 (2003).

 ©2008 The American Physical Society